13th International Brick and
Block Masonry Conference
Amsterdam, July 4-7, 2004

Finite Element Analysis of Masonry Subject to Quasi-static and Dynamic Out-of-plane Loading.

G Beattie[1], TCK Molyneaux[2], M Gilbert[3], S Burnett[4]

Abstract

The behaviour of parapet walls when subjected to vehicle impact loads is of interest worldwide. There are well-accepted analytical procedures and design guidelines for those constructed of steel, aluminium or reinforced concrete. However this is not the case for masonry parapets – many of which were constructed when dynamic loading requirements were not specifically considered.

As part of a recent project a series of tests have been completed to investigate the response of masonry specimens under both quasi-static and dynamic loading conditions (Beattie, 2003). Benchmark experimental results were obtained and LS-DYNA, a general purpose non-linear explicit finite element program, was used to try to simulate the test results. The standard software was modified so as to include an interface algorithm incorporating dilatancy and post-peak softening, to better represent the failure of the brick/mortar interface.

The influence of dilatancy and post peak softening parameters on the behaviour of masonry is investigated with reference to both the numerical analyses and the laboratory test results.

Key Words

joint, wall, finite element, softening.

[1] Senior Structural Engineer, Arup, Liverpool, UK. Email:greg.beattie@arup.com
[2]Lecturer, RMIT University, Melbourne, Australia. Email:tom.molyneaux@rmit.edu.au
[3] Lecturer, University of Sheffield, Sheffield, UK. Email: m.gilbert@sheffield.ac.uk
[4] Research Assistant, University of Sheffield, UK. Email:cip99sjb@sheffield.ac.uk

1 Introduction

In recent years there has been an increased interest in the micro-level mechanical behaviour of masonry (e.g. Rots, 1997). Various modelling strategies have been developed and implemented in finite element programs. However, work to date has tended to focus on quasi-static loading conditions whereas masonry structures may also be subjected to dynamic loads, for example, from earthquakes, blasts or vehicle impacts.

The work presented in this paper forms part of the second phase of a two-phase project concerned with the impact resistance of masonry walls. The phase one work which was completed in 1996 developed strategies for the numerical analysis of masonry bridge parapets subjected to "car like" impacts and contributed towards the development of UK standards: a County Surveyors Guidance Note (1995) and BS 6779 pt 4 (1999) which provide guidance on the design and assessment of masonry bridge parapets. The phase one work showed that there was an apparent increase in the shear and tensile strength of the brick/mortar interface bond under impact loading regimes. This apparent increase in strength had to be incorporated into the finite element models in order to obtain reasonable numerical predictions of experimental tests. Although, the reasons for this increase were never fully investigated it was thought that the mode I and mode II fracture energies, joint dilatancy and possibly features of the particular test arrangements used to determine the impact strengths of the materials were factors contributing to the (apparent) strength increase.

Recently the dynamic material behaviour has been investigated in more detail by using a series of physical tests, with results being compared to a finite element representation of masonry (Beattie, 2003). The differences between the experimental and numerical results have been quantified by analysing key laboratory tests using the finite element formulation for the brick/mortar interface adopted by Molyneaux (1995). This interface formulation has then been further developed with the aid of test data and analysis work.

As part of the test programme a series of small, medium and large-scale tests were developed. This paper describes the use of a medium scale (beam) test in validating the overall finite element modelling strategy.

2 Laboratory Test Beams

One unreinforced masonry beam and three reinforced masonry beams were tested under both quasi-static and dynamic loading.

2.1 Unreinforced Beam Test

The unreinforced beam (URB1) was 1790mm in length, 300mm high and 328mm wide constructed using English Bond (Figures 1 and 2). During construction of the beams small batches of mortar were made to ensure that each mix was used within 15 minutes of production. This helped to ensure consistency throughout the beam and ensured that the mortar was used before it became unworkable. The mix for this beam was batched using 12500g of sand, 1080g of lime, 2076g of cement, and 2725ml of water. After construction and curing the beam was rotated 90^{o} about its longitudinal axis before being placed into the test rig (Figure1). This enabled a vertically applied load to be used to approximately replicate the out-of-plane lateral load applied to a real masonry parapet wall.

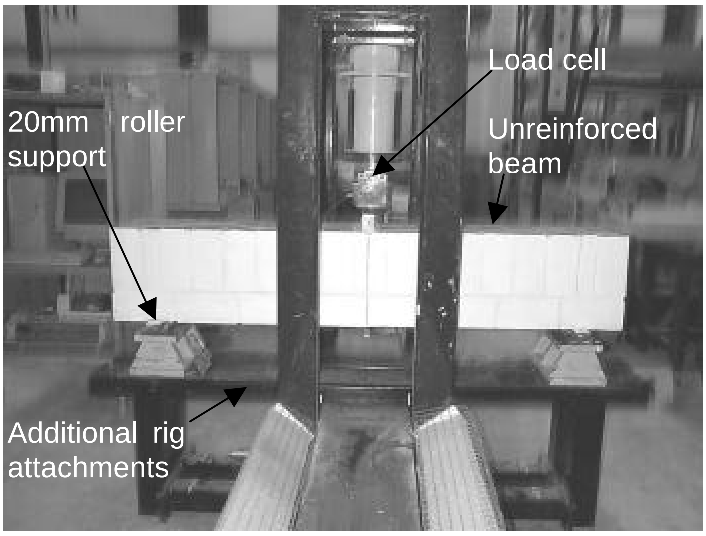

Figure 1– Unreinforced beam test arrangement

The span between supports was 1.5m with each end supported on a 20mm diameter roller (allowing rotation but no horizontal or vertical translation at the supports). The load was applied via a 50mm wide steel bar across the full width of the top of the beam (Figure 1) in 0.5kN increments until failure occurred. At each load increment, central displacements were recorded. Cracks were also monitored visually throughout loading.

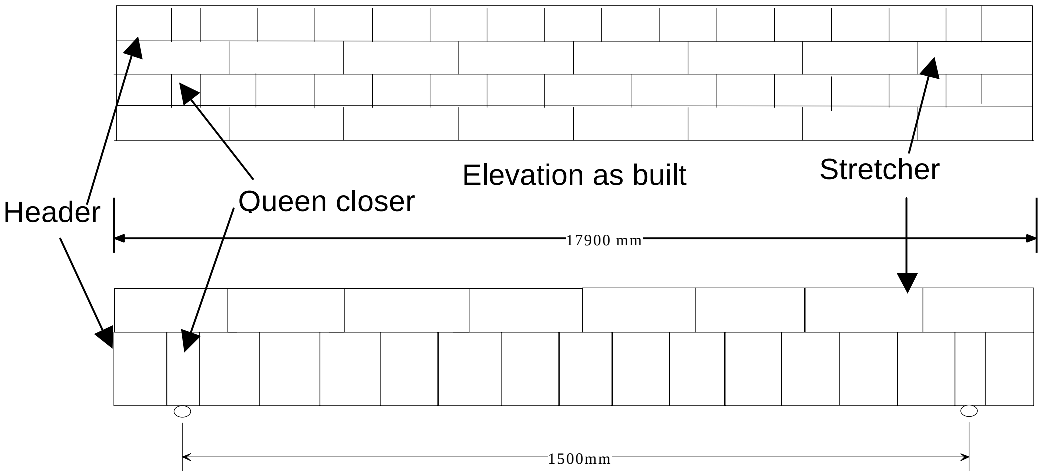

Figure 2– Beam bond pattern

2.2 Reinforced Beam Test

The reinforced beams were constructed using English Bond and were identical in size and bond pattern to URB1 described in Section 2.1. Two bars were incorporated into the tensile face and two into the compression face of each beam (positioned 50mm from the surface). Strain gauges were affixed at various positions along the length of the reinforcing bars.

Beams RB1 and RB2 were constructed and positioned in the test rig using the same procedure as for URB1. The quasi-static load was applied in increments of 1.0kN with strain readings taken from the strain gauges and displacement gauges at each load increment. A Hewlett Packard 34970A data acquisition system was used to log the strain gauge readings at each load increment. The central displacement of these two

walls was also measured manually using a displacement gauge positioned under the beam.

Beam (RB3) was tested under an impact load using a drop hammer rig (Beattie, 2003), modified so as to increase the impact mass from 23kg to 100kg to ensure failure of the beam. Figure 3 below shows the impactor.

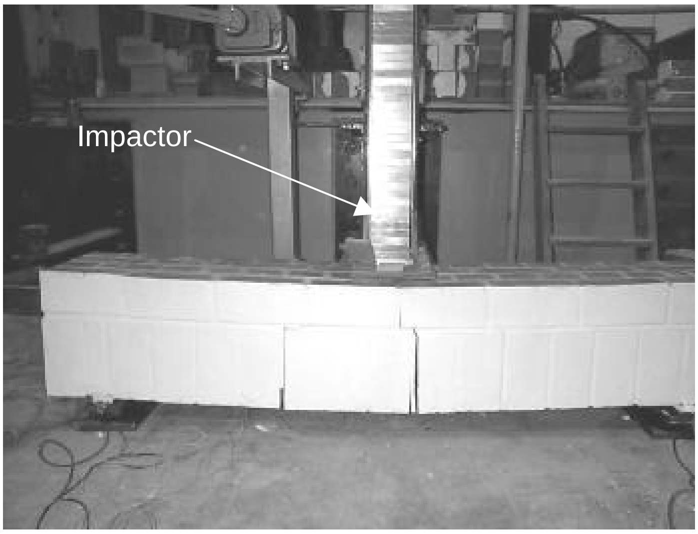

Figure 3 – RB3 after test showing impactor

Beam RB3 was constructed in the same manner as the other beams. The supports however included four Novatech F207c 100kN load cells (two at each support). These were clamped between two plates applying a small pre-load using bolts passing through the centre of the cells, but still allowing free downward movement of the top plate. The 20mm diameter roller supports were then positioned in 20mm diameter grooves cut into the top plates. The bottom plates were then positioned on the reinforced concrete strong floor at the base of the drop hammer rig. The beam was rotated and positioned on the supports. The four reaction forces and the strain gauge readings were connected to high speed logging equipment described elsewhere (Beattie, 2003).

The impactor was dropped through a height of 2m onto a load attenuator comprising 40mm of fibreboard in order to produce the required loading rate.

2.3 Test results

The results for the unreinforced beam test are shown in Figure 4. Although the test used a load control system (with load increments of 0.5 kN), when the load was held at 21kN the beam failed. Once the peak load had been reached, cracking was audible, cracks quickly propagating upwards from the soffit of the beam, eventually separating the beam into two halves.

Figures 5 and 6 show the force vs. displacement and force vs. strain graphs for the first reinforced beam test (RB1). As the displacement and strain readings were taken manually, the readings had to be stopped before ultimate failure. After removal of the instrumentation the displacements increased significantly (as the reinforcement yielded) and the beams failed completely at 3.02 tonnes and 2.8 tonnes for RB1 and RB2 respectively.

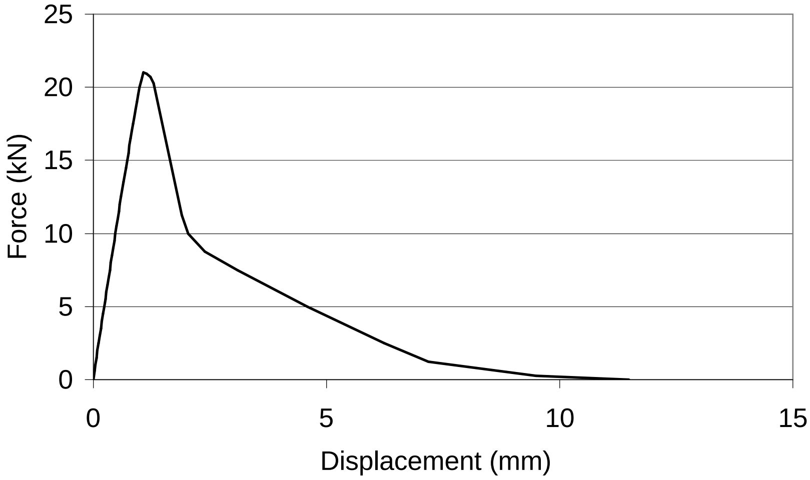

Figure 4- Force v.s. displacement for unreinforced beam

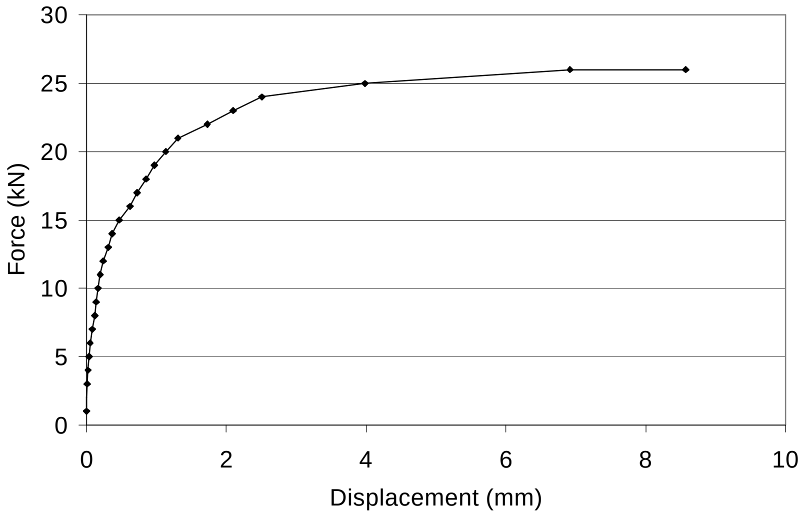

Figure.5- Force vs. displacement for reinforced beam RB1

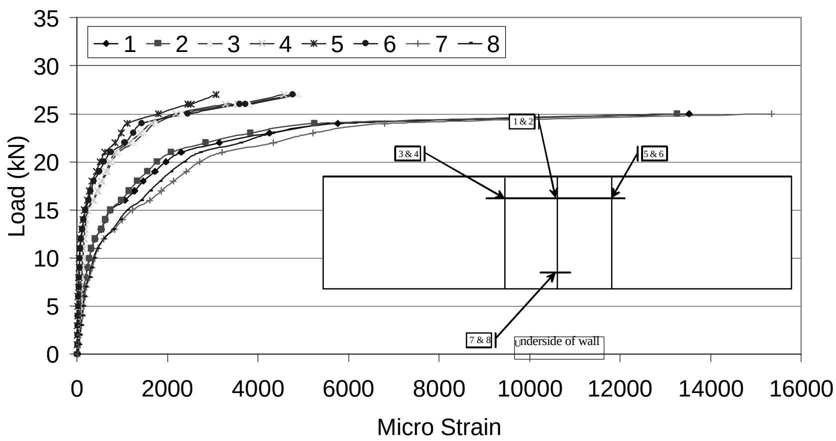

Figure 6- Force vs. strain for test RB1

Experimental and numerical force vs. time responses for reinforced beam RB3 are shown on Figure 7. This indicates that the peak load reached experimentally was 90kN, which is significantly higher than the mean quasi-static failure load of 29kN. The average strain recorded on the centre gauges was about 3000 micro-strain compared to approximately 10000 micro-strain recorded during the quasi-static tests. The impact

did not result in the beam failing completely, although significant cracks had developed (Figure 3). Displacements were not monitored throughout the test, but following the impact event the residual midspan displacement was 20mm.

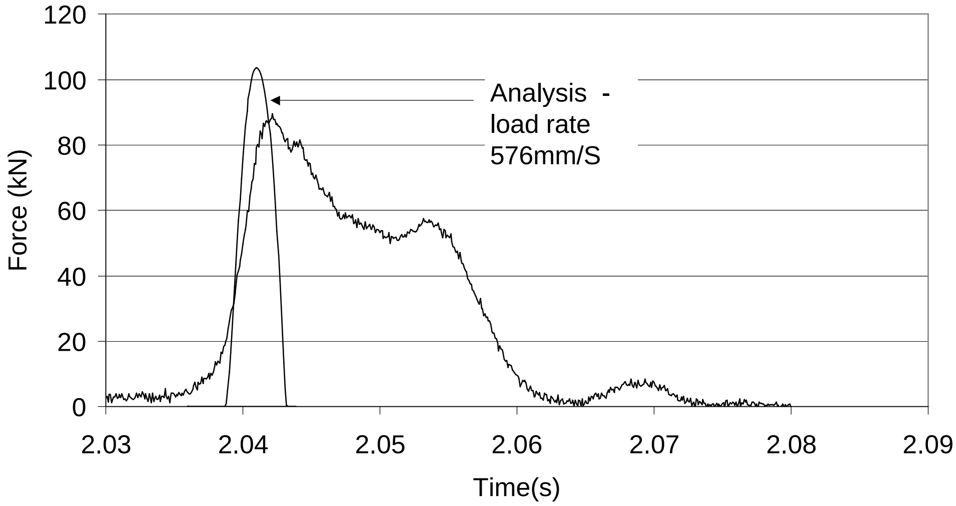

Figure 7- Force vs. time for reinforced beam RB3

3 Numerical Analysis

Molyneaux *et al* (1995) used the specialised contact surface formulation available in the explicit finite element code LS-DYNA (Hallquist, 1997) to represent masonry joints. This approach was used reasonably successfully to model brickwork and stone walls undergoing large deformations during vehicle impacts. However, to achieve good correlation between full-scale test data and the numerical results, enhanced (above normal quasi-static) values of the limiting stresses had to be adopted.

The work presented within this paper employs a modified interface formulation originally proposed by Gilbert *et al*. (1998). This model has now been incorporated into CEAP 8.0b, a version of LS-DYNA (the source code of CEAP 8.0b was made available by Ove Arup & Partners Ltd to facilitate development of a masonry specific contact interface).

The parameters considered for inclusion were:

i. Mode I fracture energy
ii. Mode II fracture energy
iii. Dilatancy
iv. Dynamic enhancement coefficient
v. Mohr Coulomb failure criteria

Material properties to describe the failure characteristics of masonry were those determined by Beattie (2003) and are shown in Table 1.

To investigate the sensitivity of the post-failure parameters, a further series of analyses was conducted. These analyses had the base values described in Table 3.1, with the following changes included:

- Low Mode I = Mode I fracture energy reduced to 0.275 mm (equivalent displacement)
- High Mode II = 1.13 mm (equivalent displacement)
- High Dilatancy , coefficient of friction (dilatant)= 0.66

Table 1 – Interface properties used for beam analysis

Parameter	Value
Limiting Shear Stress	0.63 N/mm^2
Limiting Tensile Stress	0.39 N/mm^2
Mode I Fracture Energy	0.031 N/mm
Mode II Fracture Energy	0.059 N/mm
Coefficient of friction (dilatant)	0.22
Limiting Shear Displacement	0.8 mm
Coefficient of Friction	1.65

Figure 8 shows the outline mesh used for this beam analysis. Each brick consisted of 48 elements (only 3 elements per brick are shown in Figure 8 for clarity). Interfaces were employed at all locations where a mortar bed or perpend joint would occur. In all 10 interfaces were defined in the model. Each bed joint and each longitudinal vertical joint (Figure 8) was defined individually and the perpend joints at the end of each brick were defined as a single interface. The remaining two interfaces were defined as being frictional (LS-DYNA interface type 3) and were used between the supports and the wall and the loading bar and the wall. The supports and loading platen were geometrically identical to those used for the laboratory beam tests, however they were assigned rigid material properties as it was assumed that the stiffness of these elements would not have a significant effect on the behaviour of the beam.

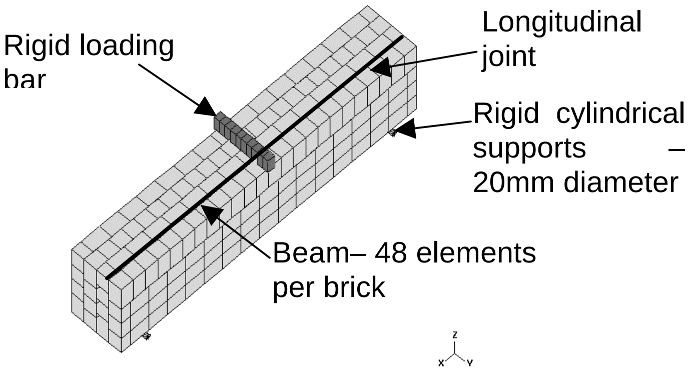

Figure 8 – Finite element model

The reinforced beam model was similar to the unreinforced beam model described above with a strip of shell elements incorporated to represent each reinforcing bar.

The shell elements adopted used the Belytschko Tsay formulation (Hallquist ,1997) which is the LS-DYNA default shell element. The material model adopted was Isotropic Elastic Plastic with properties defined as determined from laboratory tests. To simulate the behaviour of the circular ribbed reinforcing bars, one side of the shell elements was given the same surface area as the ribbed bars (18.84mm). One side of the shells was then fixed to the adjacent brick bed joints using a tied interface with failure (modified LS-DYNA interface type 9) with the following properties:

- Internal coefficient of friction for debonding of reinforcement (μ_i)= 20.12
- Limiting shear stress ($\mathbf{t}_{lim}$) = 2.76 N/mm^2 - based on the average pull-out stress from tests.
- Limiting tensile stress (s_{lim}) = 10N/mm^2

The fracture energy characteristics were as for the brick/mortar interface as currently the formulation does not allow for differentiation between different materials using the same (modified) LS-DYNA type 9 tied interface. In addition, no laboratory data was available to characterise the reinforcement/masonry failure.

Following initial analyses it was determined that the bar debonded prematurely. Therefore, a further series of analyses were conducted with an increased limiting shear stress of 10N/mm^2.

3.1 Results

Figure 9 shows the reaction force versus displacement for all of the unreinforced analyses described above, whilst Figure 10 shows the reinforced beam analysis compared to laboratory results.

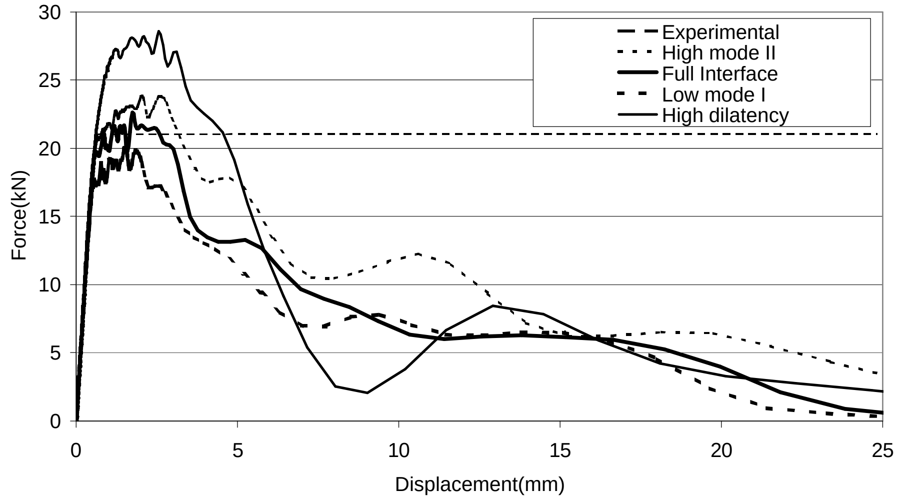

Figure 9- Analyses results of unreinforced beam analysis

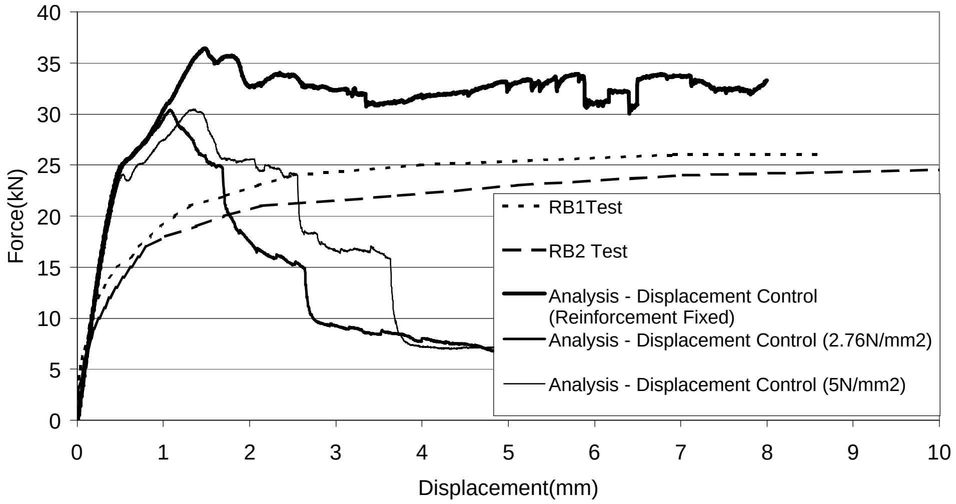

Figure 10- Force vs displacement for reinforced beams

3.2 Discussion

From Figure 9 it can be observed that when using the interface variables as shown in Table 1, the overall failure load of the beam is similar to that of the laboratory test (i.e. 22.5kN compared to 21.1kN). However, the following are not considered:

- Softening of the coefficient of friction.
- Variation of fracture energy under varying degrees of pre-compression.

- Softening of the coefficient of dilatant friction.

It has been shown by Beattie (2003) these parameters are not constants and can influence the analysis. However, when addressing the “global” behaviour the effects of these appear to be quite small.

When the mode I or mode II fracture energy is altered (by 50%) the overall “global” behaviour does not differ significantly. However, increasing the dilatancy clearly affects the analysis results. This is likely to be due to the geometric confinement (interlocking of the bricks). Whereas, for simpler numerical models such as triplet models (Beattie, 2003) there is no interlocking behaviour and only applied levels of precompression alter the behaviour of the interface, the beam is more complex and the geometric confinement creates normal compressive stresses as shear displacements are initiated. Therefore, although the average coefficient of dilatant friction value of 0.22 has been used and produces reasonable results, the more complex the model the greater the requirement for more detailed evaluation of dilatancy and the more important the inclusion of softening to this parameter becomes when trying to produce an interface formulation which allows objective modelling of masonry.

When considering Figure 10 it is observed that the similarity in failure loads between laboratory test and analytical model is only true for shear failure contact stresses between masonry and reinforcement of up to 5N/mm^2. When 10N/mm^2 is adopted the failure load increases, although the post peak behaviour trend is then similar to that observed in the laboratory tests. Only the model where 10N/mm^2 was adopted as the limiting interface stress produced any plastic strain within the reinforcement, whereas when the lower stresses were used the bar debonded before any section of the bar had reached its yield stress. It was also observed that the post yield straining occurs at a higher level of load in the numerical model.

Results from tests on the reinforced beam loaded dynamically in the drop hammer rig compared reasonably well with results from a numerical model when a similar loading gradient was applied (see Figure 7). It can be observed that the failure loads are similar, although the post-peak behaviour differs. This could be attributable to the fracture energy characteristics and dilatancy that have both been shown to have an effect on the pre and post-peak behaviour when included in numerical models, but have also been shown to be sensitive to normal compressive stresses (Beattie, 2003). As shown in the simpler triplet models (Molyneaux *et al*, 2002), the fracture energy increases under increasing precompression. Due to the high rate of loading here high levels of precompression can be observed However the increase in fracture energy due to increased levels of precompression is not represented by the current interface model and the value adopted has been shown to be unrepresentative.

It should also be noted that the crack patterns observed in the laboratory tests and the numerical models following failure were generally similar.

4.0 Conclusions

The interface formulation adopted (Gilbert *et al* 1998) can reasonably represent the pre and post peak static and dynamic behaviour of masonry by the incorporation of fracture energy, dilatancy and Mohr Coulomb failure criterion.

Although the influence of the mode I (tensile) fracture energy is not as significant as the mode II (shear) fracture energy values, it has been demonstrated by the beam model analysis that the magnitude of mode I fracture energy does affect the analysis results.

Dilatancy at the mortar interface has been shown to affect the behaviour of masonry under both quasi-static and dynamic loading regimes. However, the influence of dilatancy is more obvious when precompression is present. The effect is more dominant in larger models (i.e. beams) where geometric confinement is significant. However, to improve the efficiency and accuracy of the interface formulation, the angle of dilatancy should be allowed to vary according to the amount of shear displacement, and should also be dependent on the level of precompression.

In the numerical model the fracture energy and dilatancy behaviour associated with reinforcement debonding are by default the same as those used for the brick/mortar interface. Athough this has been shown to work reasonably well, the ability to differentiate between these is required for future work where more accurate material data on the fracture energy and dilatancy properties associated with debonding of the reinforcement are really required.

References

Beattie, G., (2003). Joint Fracture in Reinforced and Unreinforced Masonry under Quasi-Static and Dynamic Loading, PhD Thesis, Dept. of Civil Eng. University of Liverpool, UK.

BS 6779, Part 4 (1999), Highway parapets for bridges and other structures – specification for parapets of reinforced and unreinforced masonry construction.

County Surveyors' Society Guidance Note (1995). The assessment and design of unreinforced masonry vehicle parapets **1-2**. Research Report. Preston: Lancashire county Council.

Gilbert, M., Molyneaux, T.C.K., and Hobbs, B., (1998) 'A dynamic finite element modelling approach for masonry structures', Proceedings of the British Masonry Society, No. 8, pp. 182-187.

Hallquist, J.O., (1997), LS-DYNA (v940) Users Manual (Nonlinear Dynamic Analysis of Solids in Three Dimensions). Livermore Tech Corporation.

Molyneaux, T.C.K., (1995), The Assessment and Design of Unreinforced Masonry Vehicle Parapets. Vol. 2, Report No. CE/08/95, Dept of Civil Eng. University of Liverpool, UK.

Molyneaux, T.C.K, Gilbert, M. and Hobbs, B., (1995) 'Modelling vehicle impacts on freestanding masonry walls', Proc. 3rd International Symposium on Computer Methods in Structural Masonry, Lisbon.

Molyneaux, T.C.K., Beattie, G., Gilbert, M., Burnett, S., Hobbs, B., Newton, P., (2002) 'Assessment of static and dynamic failure characteristics of mortar joints in unreinforced and reinforced masonry', Proceedings of the British Masonry Society, No. 9, pp. 341-350

Rots, J.G., (1997) 'Structural Masonry: An Experimental/Numerical Basis for Practical Design Rules', AA Balkema, Rotterdam.